

Cationic ring-opening polymerization of 2-propyl-2-oxazolines: Understanding structural effects on polymerization behavior based on molecular modeling

Hannelore Goossens,[†] Saron Catak,[†] Mathias Glassner,[‡] Victor R. de la Rosa,[‡] Bryn D. Monnery,[‡] Frank De Proft,[§] Veronique Van Speybroeck,^{†,*} Richard Hoogenboom^{†,*}

[†] Center for Molecular Modeling, Ghent University, Technologiepark 903, 9052 Zwijnaarde, Belgium

[‡] Supramolecular Chemistry Group, Department of Organic Chemistry, Ghent University, Krijgslaan 281-S4, 9000 Ghent, Belgium

[§] Eenheid Algemene Chemie, Vrije Universiteit Brussel, Pleinlaan 2, 1050 Brussels, Belgium

Supporting information

Table of contents

Experimental details	S2
Materials and Instrumentation	S2
Monomer synthesis	S2
Polymerization kinetics	S2
Evolution of molecular weight (distribution) with conversion for the CROP of PropOx	S3
Preliminary B3LYP calculations	S4
Gibbs free energy profiles	S4
Electrophilicity	S5
Fukui functions	S5
Cartesian coordinates of transition states	S6
Cartesian coordinates, energy, imaginary and low frequencies of the optimized geometry (B3LYP/6-31+G(d,p)) of c-PropOx-TS.	S6
Cartesian coordinates, energy, imaginary and low frequencies of the optimized geometry (B3LYP/6-31+G(d,p)) of n-PropOx-TS.	S7
Cartesian coordinates, energy, imaginary and low frequencies of the optimized geometry (B3LYP/6-31+G(d,p)) of i-PropOx-TS.	S8
Full reference of Gaussian09	S9
References	S9

Experimental details

Materials and Instrumentation

All reagents were purchased from Sigma Aldrich and used as received, except acetonitrile and methyl tosylate. Acetonitrile was purified by distillation over barium oxide before use as polymerization solvent and methyl tosylate was purified by distillation over barium oxide and stored under argon.

Polymerizations were performed in capped vials in a single mode microwave reactor Anton Paar Monowave 300 (IR sensor for temperature control) equipped with a MAS24 autosampler. The vials were heated to 130 °C for at least two hours, and cooled down under argon before usage.

SEC was measured on a Agilent 1260-series HPLC system equipped with a 1260 online degasser, a 1260 ISO-pump, a 1260 automatic liquid sampler (ALS), a thermostatted column compartment (TCC) at 50 °C equipped with a PSS Gram30 column in series with a PSS Gram1000 column (Pn-PropOx and Pi-PropOx) or two Agilent mixed D columns in series (Pc-PropOx), a 1260 diode array detector (DAD) and a 1260 refractive index detector (RID). The used eluent was DMA containing 50mM of LiCl at a flow rate of 1ml/min. The spectra were analysed using the Agilent Chemstation software with the GPC add on. Molar mass and PDI values were calculated against Varian PS standards.

Gas chromatography was performed on 7890A from Agilent Technologies with an Agilent J&W Advanced Capillary GC column (30 m, 0.320 mm, and 0.25 µm). Injections were performed with an Agilent Technologies 7693 auto sampler. Detection was done with a FID detector. Injector and detector temperatures were kept constant at 250 and 280 °C, respectively. The column was initially set at 50 °C, followed by two heating stages: from 50 °C to 100 °C with a rate of 20 °C /min and from 100 °C to 300 °C with a rate of 40 °C /min, and then held at this temperature for 0.5 minutes. Conversion was determined based on the integration of monomer peaks using acetonitrile as internal standard.

Monomer synthesis

The c-PropOx, n-PropOx and i-PropOx monomers were prepared following the previously reported synthetic procedure for c-PropOx by direct condensation of the corresponding nitriles with 2-aminoethanol.¹

In brief, the nitrile (1 equiv) and zincacetate dehydrate (catalyst, 0.02 equiv) were heated to 130 °C under reflux conditions, and 2-aminoethanol (1.1 equiv) was added dropwise. After overnight refluxing, the reaction mixture was cooled to room temperature, and dichloromethane was added. The organic phase was washed 3 times with water and once with brine. After removing the dichloromethane under reduced pressure, the monomer was purified by fractional distillation over barium oxide.

Polymerization kinetics

The polymerization kinetics were studied by preparing a stock solution of the polymerization mixture with 4 M monomer concentration in acetonitrile and methyl tosylate as initiator resulting in a monomer to initiator ratio of 50. This stock solution was divided over several microwave vials (1 mL each) that were heated for different times to 140 °C. After microwave polymerization, the mixture was cooled to 38 °C and quenched by the addition of water.

GC and SEC samples were prepared from these quenched polymerization mixtures to determine the monomer conversion and the molar mass (distribution) of the resulting polymers. The monomer conversion was calculated from integration of the GC signals, whereby the acetonitrile signal was used as internal standard.

Evolution of molecular weight (distribution) with conversion for the CROP of PropOx

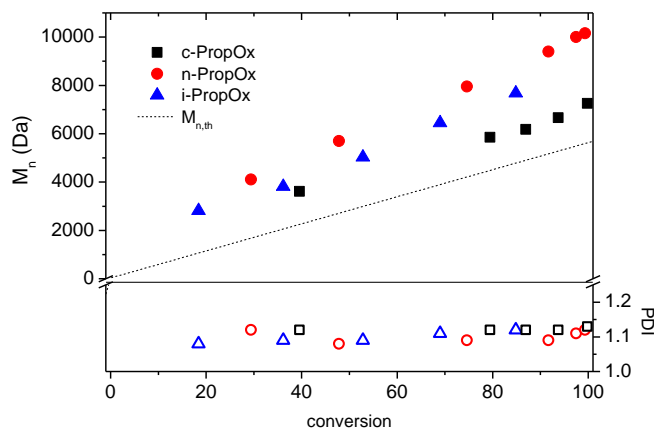
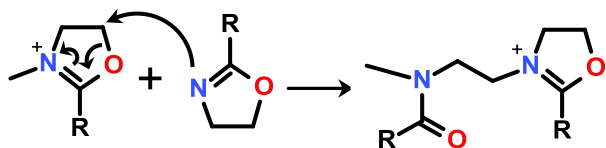


Figure S1. Number average molecular weight (M_n) and polydispersity index (PDI) as function of conversion for the CROP of 2-cyclopropyl-2-oxazoline (c-PropOx), 2-n-propyl-2-oxazoline (n-PropOx) and 2-isopropyl-2-oxazoline (i-PropOx). Polymerizations performed at 140 °C in acetonitrile with 4 M monomer (M) concentration, methyl tosylate (I) as initiator and a [M]:[I] ratio of 50. The dotted line shows the theoretical number average molecular weight ($M_{n,\text{th}}$). All polymers show narrow molecular weight distributions with PDI < 1.20. SEC of poly(c-PropOx) was measured with chloroform as eluent while the other polymers were measured with DMA as eluent, which explains the observed difference in M_n due to the different hydrodynamic radii. C-PropOx data from ref 1.



Scheme S1. Schematic representation of the modeled reaction of methyl-oxazolinium species with 2-oxazoline monomers.

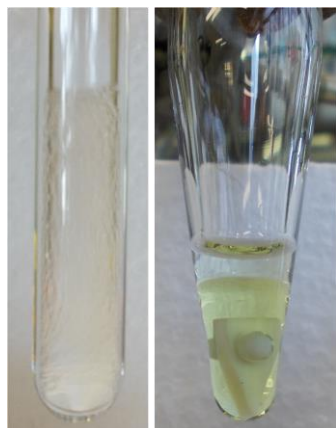


Figure S2. Photographs of the polymerization mixture of c-PropOx at 140 °C in a pressure reaction tube (left) and in a microwave polymerization tube after cooling back to 40 °C (right) clearly demonstrating that phase separation only occurs upon cooling.

Preliminary B3LYP calculations

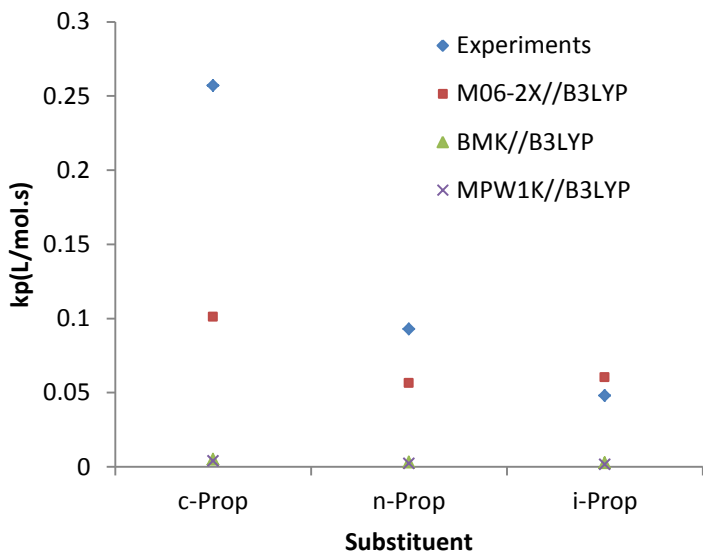


Figure S3. Comparison of experimental and calculated (B3LYP/6-31+G(d,p) optimizations, energy refinement with Mo6-2X, BMK² and MPW1K³ and a 6-31++G(d,p) basis set) rate constants of the first propagation step of the CROP of c-PropOx, n-PropOx and i-PropOx.

Gibbs free energy profiles

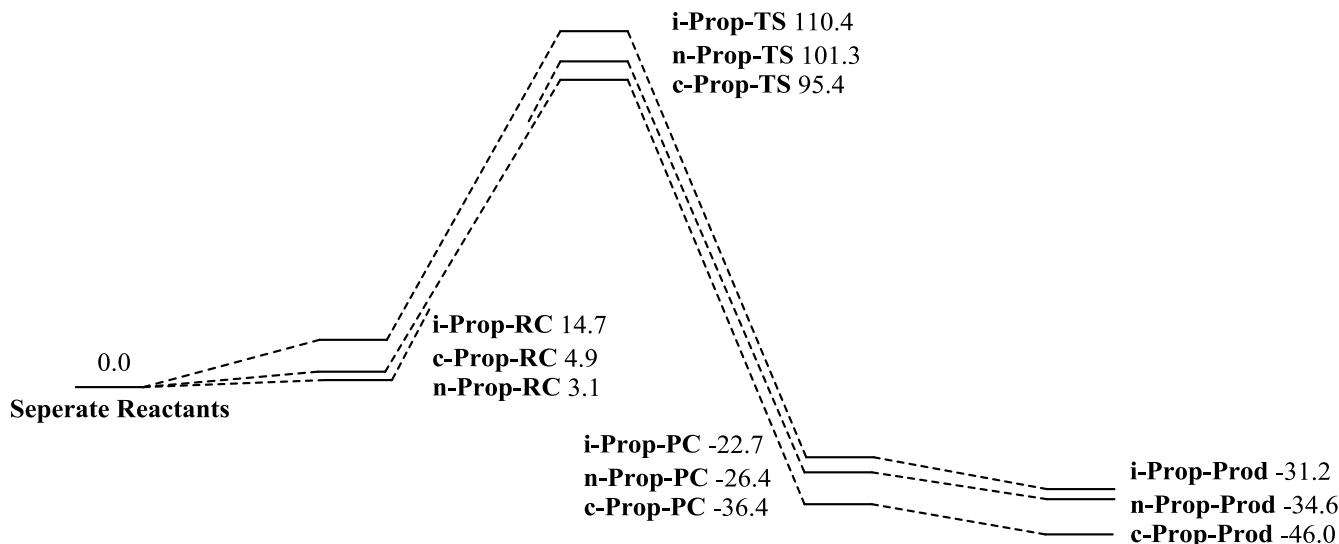


Figure S4. Gibbs free energy profiles for the first propagation step of the CROP of c-PropOx, n-PropOx and i-PropOx (Mo6-2X/6/31++G(d,p)). Energies for each different substituent relative to its own reactants. RC, TS, PC and Prod denote respectively reactant complex, transition state, product complex and product. Free energies in kJ/mol at 140°C and 1 atm. BSSE corrections were taken into account.

Electrophilicity

The electrophilicity ω can be defined as:

$$\omega = \frac{\chi^2}{2\eta} \text{ with the electronegativity } \chi = \frac{\text{IP} + \text{EA}}{2}$$

Fukui functions

Fukui functions corresponding to nucleophilic and electrophilic attack, respectively:

$$f^+(r) \approx \rho_{N+1}(r) - \rho_N(r) \approx \rho_{\text{LUMO}}(r)$$

$$f^-(r) \approx \rho_N(r) - \rho_{N-1}(r) \approx \rho_{\text{HOMO}}(r)$$

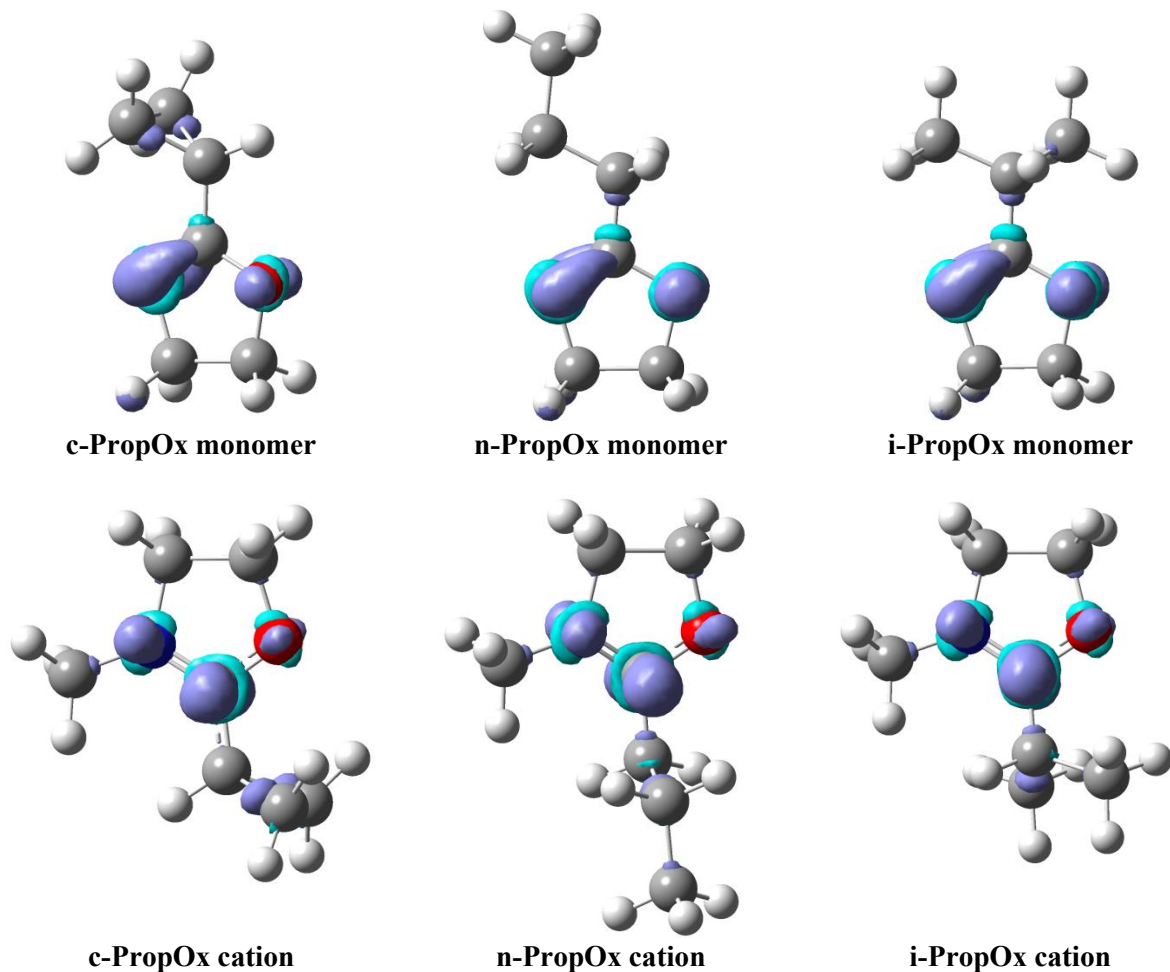


Figure S5. Electrophilic Fukui functions [isovalue 0.01 au] on oxazoline monomers (top) and nucleophilic Fukui functions [isovalue 0.01 au] on oxazoline cations (bottom).

Cartesian coordinates of transition states

Cartesian coordinates, energy, imaginary and low frequencies of the optimized geometry (B3LYP/6-31+G(d,p)) of c-PropOx-TS.

C	0.004966	-0.016050	-0.003785
C	-0.005317	0.007587	1.537040
N	1.424822	0.016445	1.872565
C	2.095266	0.203706	0.789086
O	1.383888	0.275490	-0.338888
C	3.544789	0.345157	0.670847
C	4.093346	1.236412	-0.429865
C	4.226571	-0.236781	-0.556695
C	2.043577	0.131243	3.769007
C	2.372832	-1.357852	3.806008
N	2.744840	-1.749997	5.163230
C	2.863739	-0.725888	6.012416
O	2.570007	0.411400	5.553850
C	3.066565	-3.146548	5.423496
C	3.302542	-0.889873	7.402843
C	2.628702	0.002613	8.435761
C	4.023573	0.292527	8.030650
H	2.772866	0.866762	3.466327
H	1.052555	0.481787	4.021398
H	3.195193	-1.582162	3.116970
H	1.501229	-1.939322	3.493121
H	4.119968	-3.357213	5.215418
H	2.445755	-3.769112	4.776675
H	2.835662	-3.404705	6.455982
H	3.607322	-1.879925	7.713365
H	4.082277	0.314316	1.611380
H	-0.500244	-0.868524	1.964479
H	-0.482969	0.906661	1.940698
H	-0.233134	-0.997928	-0.417446
H	-0.620111	0.745981	-0.466833
H	1.850470	0.657406	8.061019
H	2.445702	-0.449919	9.402845
H	4.192501	1.144807	7.382957
H	4.827735	0.043568	8.712487
H	3.364496	1.734161	-1.058764
H	4.969770	1.819250	-0.173243
H	3.587335	-0.741603	-1.271772
H	5.197409	-0.688723	-0.391876

Energy (mo6-2X/6-31++G**) = -767.370114 hartree

Frequencies(cm-1): -569.3206, 13.6330, 26.3640,...

Cartesian coordinates, energy, imaginary and low frequencies of the optimized geometry (B3LYP/6-31+G(d,p)) of n-PropOx-TS.

C -0.009912 0.006970 -0.011626
 O -0.008205 -0.012675 1.320214
 C 1.372457 -0.024636 1.760011
 C 2.168802 0.210956 0.460390
 N 1.138044 0.094770 -0.582372
 C -1.348250 -0.040175 -0.666882
 C -2.195688 1.186982 -0.285361
 C -1.553085 2.498656 -0.728734
 C 1.555310 0.524635 -2.488204
 C 1.654996 -0.951266 -2.862747
 N 2.071293 -1.079916 -4.256389
 C 2.203395 0.081361 -4.901220
 O 1.972844 1.116228 -4.230572
 C 2.261491 -2.415209 -4.799215
 C 2.607488 0.153152 -6.348773
 C 2.705765 1.585245 -6.873062
 C 3.116730 1.603402 -8.343044
 H 0.621379 1.062371 -2.553537
 H 2.418978 1.062720 -2.124129
 H 0.686865 -1.444325 -2.724158
 H 2.384967 -1.453282 -2.220590
 H 1.324487 -2.977160 -4.746170
 H 3.028861 -2.942917 -4.226068
 H 2.578301 -2.356018 -5.838536
 H 3.570092 -0.362334 -6.461510
 H 1.878806 -0.420633 -6.936134
 H -1.845557 -0.959956 -0.342187
 H -1.211573 -0.091833 -1.751300
 H 2.956459 -0.531642 0.310253
 H 2.619984 1.207550 0.417778
 H 1.564813 -0.999506 2.210800
 H 1.493286 0.760455 2.504954
 H 3.428315 2.140836 -6.267929
 H 1.741052 2.083868 -6.740246
 H -3.177963 1.071217 -0.751285
 H -2.352904 1.185451 0.797162
 H 3.186331 2.628349 -8.712735
 H 4.092690 1.129804 -8.488217
 H 2.388867 1.073380 -8.965257
 H -2.181730 3.350628 -0.462300
 H -0.577570 2.651361 -0.252504
 H -1.409505 2.522112 -1.814755

Energy (mo6-2X/6-31++G**) = -769.8265249 hartree

Frequencies(cm-1): -568.6547, 17.0975, 26.0295,...

**Cartesian coordinates, energy, imaginary and low frequencies of the optimized geometry
(B3LYP/6-31+G(d,p)) of i-PropOx-TS.**

C	0.006764	0.007432	0.008128
C	-0.006764	0.051953	1.550525
N	-1.442743	0.036160	1.867725
C	-2.101243	-0.138512	0.777586
O	-1.382502	-0.211628	-0.340934
C	-3.584111	-0.273559	0.628786
C	-3.925250	-1.660389	0.064420
C	-4.124192	0.849058	-0.267778
C	-2.083258	-0.093719	3.751769
C	-2.424016	1.392383	3.801686
N	-2.909123	1.748788	5.132688
C	-2.969911	0.725318	5.988645
O	-2.610260	-0.390365	5.539603
C	-3.234202	3.144213	5.381951
C	-3.388947	0.888173	7.429424
C	-3.866422	-0.445325	8.002698
C	-2.191851	1.445623	8.220724
H	-1.094860	-0.445388	4.011277
H	-2.811291	-0.828184	3.440756
H	-1.536003	1.989159	3.569377
H	-3.194757	1.630143	3.060567
H	-2.336784	3.761494	5.277118
H	-3.986116	3.480793	4.662468
H	-3.630662	3.268596	6.387258
H	-4.212706	1.609113	7.467360
H	-4.015290	-0.175491	1.631497
H	0.477919	-0.819716	2.001361
H	0.465125	0.954246	1.948428
H	0.588245	-0.815159	-0.406395
H	0.315228	0.949330	-0.448096
H	-4.179769	-0.300442	9.038941
H	-3.062109	-1.183821	7.980533
H	-4.712591	-0.845967	7.439894
H	-5.010085	-1.764802	-0.009500
H	-3.546644	-2.462655	0.703944
H	-3.498498	-1.780680	-0.934469
H	-2.479992	1.581292	9.265523
H	-1.845104	2.408920	7.835027
H	-1.357793	0.738568	8.187964
H	-5.212067	0.772017	-0.330813
H	-3.713897	0.761822	-1.276839
H	-3.872115	1.839085	0.123683

Energy (mo6-2X/6-31++G**) = -769.8287228 hartree

Frequencies(cm-1): -566.2449, 23.7533, 32.4007,...

Full reference of Gaussian09

M. J. Frisch, G. W. Trucks, H. B. Schlegel, G. E. Scuseria, M. A. Robb, J. R. Cheeseman, G. Scalmani, V. Barone, B. Mennucci, G. A. Petersson, H. Nakatsuji, M. Caricato, X. Li, H. P. Hratchian, A. F. Izmaylov, J. Bloino, G. Zheng, J. L. Sonnenberg, M. Hada, M. Ehara, K. Toyota, R. Fukuda, J. Hasegawa, M. Ishida, T. Nakajima, Y. Honda, O. Kitao, H. Nakai, T. Vreven, J. A. Montgomery, Jr., J. E. Peralta, F. Ogliaro, M. Bearpark, J. J. Heyd, E. Brothers, K. N. Kudin, V. N. Staroverov, T. Keith, R. Kobayashi, J. Normand, K. Raghavachari, A. Rendell, J. C. Burant, S. S. Iyengar, J. Tomasi, M. Cossi, N. Rega, J. M. Millam, M. Klene, J. E. Knox, J. B. Cross, V. Bakken, C. Adamo, J. Jaramillo, R. Gomperts, R. E. Stratmann, O. Yazyev, A. J. Austin, R. Cammi, C. Pomelli, J. W. Ochterski, R. L. Martin, K. Morokuma, V. G. Zakrzewski, G. A. Voth, P. Salvador, J. J. Dannenberg, S. Dapprich, A. D. Daniels, O. Farkas, J. B. Foresman, J. V. Ortiz, J. Cioslowski, and D. J. Fox *Gaussian 09, Revision B.01*; Gaussian, Inc.: Wallingford, CT, 2010.

References

- (1) Bloksma, M. M.; Weber, C.; Perevyazko, Y.; Kuse, A.; Baumgärtel, A.; Vollrath, A.; Hoogenboom, R.; Schubert, U. S., *Macromolecules* **2011**, *44*, 4057.
- (2) Boese, A. D.; Martin, J. M. L. *J. Chem. Phys.* **2004**, *121*, 3405.
- (3) (a) Lynch, B. J.; Fast, P. L.; Harris, M.; Truhlar, D. G. *J. Phys. Chem. A* **2000**, *104*, 4811. (b) Lynch, B. J.; Zhao, Y.; Truhlar, D. G. *J. Phys. Chem. A* **2003**, *107*, 1384.